Similarity-driven Topology Optimization for Statics and Crash via Energy Scaling Method

Muhammad Yousaf, Duane Detwiler, Fabian Duddeck, Stefan Menzel, Satchit Ramnath, Nate Zurbrugg, Mariusz Bujny

2023

Preprint:

This is an accepted article published in ASME Journal of Mechanical Design (JMD). The final authenticated version is available online at: https://doi.org/10.1115/1.4062943

Similarity-driven Topology Optimization for Statics and Crash via Energy Scaling Method

Muhammad Salman Yousaf
Technical University of Munich
Arcisstr. 21, 80333 Munich, Bavaria, Germany
Email: salman.yousaf@tum.de

Duane Detwiler
Honda Development & Manufacturing of America
21001 OH-739, 43067 Raymond, OH, USA

Fabian Duddeck
Technical University of Munich
Arcisstr. 21, D-80333 Munich, Germany
Email: duddeck@tum.de

Stefan Menzel
Honda Research Institute Europe GmbH
Carl-Legien-Straße 30, 63073 Offenbach/Main, Germany
Email: stefan.menzel@honda-ri.de

Satchit Ramnath
The Ohio State University
281 W Lane Ave, 43210 Columbus, OH, USA

Nathan Zurbrugg
Honda Development & Manufacturing of America
21001 OH-739, 43067 Raymond, OH, USA

Mariusz Bujny
Honda Research Institute Europe GmbH
Carl-Legien-Straße 30, 63073 Offenbach/Main, Germany

Topology Optimization (TO) is used in the initial design phase to optimize certain objective functions under given boundary conditions by finding suitable material distributions in a specified design domain. Currently available methods in industry work very efficiently to get topologically-optimized design concepts under static and dynamic load cases. However, conventional methods do not address the designer's preferences about the final material layout in the optimized design. In practice, the final design might be required to have a certain degree of local or global structural similarity with an already present good reference design because of economic, manufacturing and assembly limitations or the desire to re-use parts in different systems. In this article, a heuristic Energy Scaling Method (ESM) for similarity-driven TO under static as well as dynamic loading conditions is presented and thoroughly evaluated. A 2D cantilever beam under static point load is used to show that the proposed method can be coupled with gradient-based and also heuristic, non-gradient methods to get designs of varying similarity w.r.t. a reference design. Further testing of the proposed method for similarity-driven TO on a 2D crash test case and a large-scale 3D hood model of a car body indicates the effectiveness of the method for a wide range of problems in the industry. Finally, the application of similarity-driven TO is further extended to show that ESM also has the potential for sensitivity analysis of performance w.r.t. the extension of design domain.

1 INTRODUCTION

As the technology is advancing and computational power is increasing, structural Topology Optimization (TO) [1] is getting more and more acceptance in industry. A topologically-optimal design uses the available material efficiently and delivers the best performance under

given boundary conditions (BCs). Commonly considered objectives for TO are compliance and absorbed energy under static and non-linear dynamic loading conditions, respectively.

Out of different available approaches for TO, very widely used ones are density-based methods, including homogenization method [2] and Solid Isotropic Material with Penalization (SIMP) [3]. Another group comprises Level Set Methods (LSMs) [4]. When it comes to finding the solutions of TO problems, Optimality Criteria (OC)-based SIMP [1] is a very efficient algorithm which uses the gradient information of the considered objective function and the constraints. The unavailability of the gradient information in highly non-linear dynamic problems limits the use of OC-based SIMP to TO under static load cases. Apart from approaches using linear approximations of non-linear loads [5, 6], to address this drawback, non-gradient TO methods, e.g. Bi-directional Evolutionary Structural Optimization (BESO) approaches [7], Hybrid Cellular Automata (HCA) techniques [8, 9], and State-Based Representation (SBR) approaches [10] have been developed. The heuristic HCA makes use of the assumption that uniform distribution of the internal energy results in a topologically-optimal design. Recently, Evolutionary and Kriging-Guided Level Set Methods (EA-LSM [11] and KG-LSM [12]) were proposed as general approaches to solve TO problems under static and crash load cases.

The conventional TO methods are used successfully in industry, and problems related to manufacturing and economic performance of the optimized designs are intensively studied in the research community. On the one hand, in the past years, a significant progress has been made in integrating manufacturing constraints into standard, density-based TO and LSMs [13]. On the other hand, novel design parametrizations used in explicit TO techniques [14, 15, 16] allow for incorporation of design limitations already on the representation level. Mechanisms such as length scale control [17], structural complexity control [18], or handing of constraints for additive manufacturing [19, 20], can be also integrated into such approaches to improve manufacturability and cost efficiency. Moreover, the geometric features of the elementary components comprising the design can be modified to meet the requirements of a specific manufacturing technology [21, 22, 23, 24]. However, despite the high practical value of such methods, it is still difficult to explicitly control the final layout of the optimized structure, especially for the design requirements that cannot be easily described in a closed mathematical form, which is often the case in real-world industrial applications [25]. In our opinion, the designer should be able to flexibly steer the TO process by imposing similarity to certain reference designs because of practical reasons as discussed below.

Firstly, it is usually desired to re-use the already present optimized parts as much as possible because of economic restrictions associated with manufacturing and assembly processes. It is very common in the automotive industry to share the platform part in different models of the same vehicle with slight alterations. As a practical scenario, there might be an already present good design which was optimized subject to certain loading conditions. If the loading conditions are changed slightly, the use of the previous design might show worse performance. Although running the TO subject to the new loading conditions will improve the performance, it might deliver a completely new design. Therefore, similarity-driven TO should be used to keep the consistency with the previous design, while being able to improve the performance for the new loading conditions.

Secondly, computational cost can be reduced significantly by using similarity-driven TO in particular cases. In a specific scenario, re-optimization will be needed if a new load case is added to already applied high number of load cases. If the relative magnitude of the new load case is small, it will not modify the previously optimized topology significantly. The conventional way will require to re-run the TO subject to all the load cases, which will be computationally very costly. On the other hand, similarity-driven TO allows the designer to run the TO subject to just the newly added load case and control its similarity w.r.t. already optimized topology.

Thirdly, similarity-driven TO can help in the easier re-integration of topologically-optimized structural components into a bigger system. TO of these components is performed in the initial design phase and their re-integration into the bigger system is a challenge, for example, due to the required but not structurally significant connection locations on the base part that are eliminated by the TO. This limits the types of structural topology allowed for these components. Similarity-driven TO makes the re-integration easy by enabling the designer to express his or her desires at the start of the TO process about the final obtained structural layout.

Finally, as discussed in [26] and [27], novelty in some structural components is also inevitable in the product development phase. To make the product stand out in a big crowd, both performance as well as good aesthetics and novelty are important. Similarity-driven TO discussed in this paper is able to deliver the optimized design by controlling either the similarity or dissimilarity w.r.t. a reference as specified by the designer. By imposing high dissimilarity to the reference, the optimization can be guided towards novel solutions, if novelty [27] is interpreted through geometric dissimilarity.

Very little discussion is available in literature about similarity-driven TO. By coupling generative design exploration [28] with deep neural network generative models and OC-based SIMP TO, in [26], a framework to obtain designs with better aesthetics using already available reference designs has been developed. The first component of this framework is *iterative design exploration*, which generates a large number of designs using TO and deep generative models. The second component, *design evaluation*, evaluates the designs on the basis of novelty and other user-specified attributes. Even though the approach is effective to get the desired structural layout, the unavailability of sensitivity information and complexity of the iterative design exploration phase hinders its application to highly non-linear dynamic scenarios and large-scale industrial problems. Recently, we proposed four novel approaches for similarity-driven TO: Energy Scaling Method (ESM), OC-based SIMP with similarity constraint, weak passive material method, and modified design domain method [25]. The initial experiments showed that ESM is the most promising approach for similarity-driven TO.

In this article, we present an extensive analysis of ESM, including application to a large-scale industrial problem, and propose novel extensions of this approach. First of all, we rigorously compare ESM to a formal, gradient-based SIMP method with a similarity constraint and quantify the differences between both approaches. We demonstrate the universality of ESM by integrating it with both OC-based SIMP and heuristic HCA method. In a set of benchmark 2D dynamic crash problems, we evaluate the sensitivity of the method w.r.t. different impact velocities. Secondly, we apply ESM to a real-world hood frame TO problem with a similarity target, which is a novel problem formulation, and demonstrates the efficiency and the potential impact of this approach in the industrial setting. Furthermore, we propose and evaluate ESM for a new problem of subdomain similarity, which allows controlling the structural layout locally. In addition, we find the key determinants of the relationship between the parameters of ESM and the final optimization result based on a sensitivity study using four different reference structures in a 2D static scenario. Finally, we show the potential of applying ESM to the problem of design domain extension, which, to the best of our knowledge, is a problem not addressed so far in the TO research, but could play a very important role in the industrial context.

2 OBJECTIVE FUNCTIONS IN TO

The type of objective function in TO depends on the kind of loading conditions which the structure is required to support. Usually, for static load cases, the objective function in TO is the overall compliance of the structure. TO delivers the final design with minimum compliance (maximum stiffness) and this is referred to as compliance minimization problem. A typical SIMP-based compliance minimization TO problem subject to a volume fraction constraint can be described as follows [29]:

$$\begin{aligned} \min_{\mathbf{x}} \quad & c(\mathbf{x}) = \mathbf{U}^{\mathrm{T}}\mathbf{K}\mathbf{U} = \sum_{e=1}^{N} (x_e)^P \mathbf{u}_{\mathrm{e}}^{\mathrm{T}} \mathbf{k}_{\mathrm{e}} \mathbf{u}_{\mathrm{e}}, \\ \text{s.t.} \quad & \frac{V(\mathbf{x})}{V_0} = f, \;\; \mathbf{K}\mathbf{U} = \mathbf{F}, \;\; \mathbf{0} < \mathbf{x}_{\min} \leq \mathbf{x} \leq \mathbf{1}. \end{aligned} \tag{1}$$

In Eq. (1), c is the overall compliance of the structure. $\mathbf{U}$, $\mathbf{K}$, and $\mathbf{F}$ are global displacement vector, stiffness matrix, and force vector, respectively. Similarly, $\mathbf{u}_{\mathrm{e}}$ is the elemental displacement vector while $\mathbf{k}_{\mathrm{e}}$ is the elemental stiffness matrix. N is the total number of finite elements in the design domain and V, V_0 are the volume occupied by material and total design domain, respectively. Moreover, $\mathbf{x}$ is the vector containing the relative mass density of each element w.r.t. the base material. A non-zero $\mathbf{x}_{\min}$ is specified to avoid singularity, while P represents penalization and f is the prescribed volume fraction.

On the other hand, for non-linear dynamic loading scenarios like impact loading, it is required by the structure to deform in a controlled way to absorb the maximum amount of energy. In fact, this is contradictory to the compliance minimization problem mentioned above. Plastic strains are quite large in impact loading and they are used to calculate the total absorbed energy. As discussed in [30], the total absorbed energy density (or internal energy density IED) during the impact is a sum of elastic strain energy density (SED) U^e and inelastic strain energy density or plastic work U^p, i.e., $IED = U^e + U^p$. Analogous to Eq. (1), based on [30], the optimization problem for crash can be described as follows:

$$\begin{aligned} \min_{\mathbf{x}} \quad & \frac{1}{IED(\mathbf{x}, t = t_{final})}, \\ \text{s.t.} \quad & \frac{V(\mathbf{x})}{V_0} = f, \;\; \mathbf{R}(t) = \mathbf{0}, \;\; \mathbf{0} < \mathbf{x}_{\min} \leq \mathbf{x} \leq \mathbf{1}. \end{aligned} \tag{2}$$

where $\mathbf{R}(t) = \mathbf{0}$ denotes dynamic equilibrium at time t.

Besides the maximum absorbed energy, peak force/acceleration, and maximum intrusion are also very important for the crashworthiness of a vehicle. As discussed in [31], the energy absorbing behavior of two vehicles having the same mass can be quite different. One

can absorb an energy E with high peak force and low intrusion (*stiff design*), while other can absorb the same energy E with low peak force, but high intrusion (*flexible design*). A good design obtained after TO offers a fair compromise between stiffness and flexibility.

3 GEOMETRIC SIMILARITY METRICS

The level of geometric similarity between mechanical parts can be quantified in many different ways, depending on the geometric properties of the design that are of interest [32]. At the most general level, the designs can be compared in terms of macroscopic properties such as volume, size, overall shape, or topology. Hand-engineered geometric features such as statistics of material distribution, curvature, or spectral descriptors [33], are also used to quantify geometric differences between 3D objects. Recently, several data-driven methods for quantifying geometric differences among topologically-optimized designs have been evaluated in the context of design clustering [32], as well. Although these methods are very promising, they rely on availability of a large number of designs to extract relevant geometric features and are difficult to interpret. Hence, in this paper, we use a dissimilarity metric s being a mean squared difference between the elemental relative densities of the obtained design and the reference design [25, 26]:

$$s = \frac{\sum_{e=1}^{N} \left(x_e - x_e^{ref}\right)^2}{N}, \tag{3}$$

where N, x_e, and x_e^{ref} represent the total number of elements, relative density of element e in the obtained design, and relative density of the element e in the given reference design, respectively. The proposed metric has an intuitive interpretation, and by incorporating it into the optimization process, one can control much finer structural details of the design than with macroscopic properties such as volume or size.

4 ENERGY SCALING METHOD (ESM)

In [25], we implemented an extra similarity constraint along with the conventional volume fraction constraint directly in OC-based SIMP for 2D compliance minimization. This can be regarded as a formal mathematical method for similarity-driven TO. Here, similarity-driven TO is realized by using the sensitivity information of the objective function (compliance) and the constraints, including the dissimilarity metric s given by Eqn. (3).

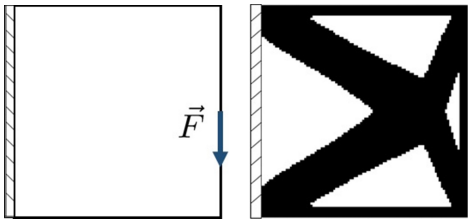

(a) Design domain with BCs.

(b) Reference design. Preferred region (black) and the non-preferred one (white).

Fig. 1: Representation of the preferred and non-preferred regions in ESM [25].

Since OC-based SIMP requires sensitivities of objectives and constraints, it cannot be used for crash cases. It is discussed in [25] that the implementation of the similarity constraint in OC-based SIMP is in fact equivalent to the scaling of elemental strain energies. If the strain energy in a design domain region is scaled up artificially, more material will be deposited from the surrounding to that particular region in the subsequent TO iterations. Taking inspiration from this formal approach, a novel non-gradient heuristic Energy Scaling Method (ESM) is introduced in [25], which can be coupled with gradient-based methods like OC-based SIMP or non-gradient methods like HCA for similarity-driven TO. To implement ESM, the design domain is divided into the following two subdomains, based on the material distribution in the given reference design (Fig. 1):

Preferred subdomain: Subdomain which must have a maximum amount of available material to obtain maximum similarity w.r.t. the reference design.
Non-preferred subdomain: Subdomain which must have a minimum amount of material to obtain maximum similarity w.r.t. the reference design.

To achieve designs similar to the reference, ESM scales up the elemental energies in the preferred region and scales down the elemental energies in the non-preferred regions. This is realized by applying a scaling factor p and $1-p$ to the elemental energies in the preferred and non-preferred region, respectively. In the OC-based SIMP for compliance minimization, the elemental energies are proportional to the corresponding compliance sensitivities $\partial c/\partial \mathbf{x}$, where c and $\mathbf{x}$ are the overall compliance and the elemental relative densities vector, respectively. On the other hand, in HCA, a designated field variable, strain energy density (SED), is available for applying energy scaling. The incorporation of ESM in OC-

based SIMP and HCA is summarized in Table 1 and the flowchart in Fig. 2.

Table 1: ESM for similarity-driven TO using OC-based SIMP and HCA [25]. P denotes the preferred region (zone) and NP the non-preferred one.

Zone	OC-based SIMP	HCA
P	$\frac{\partial c}{\partial \mathbf{x}} := p \cdot \frac{\partial c}{\partial \mathbf{x}}$	$SED := p \cdot SED$
NP	$\frac{\partial c}{\partial \mathbf{x}} := (1-p) \cdot \frac{\partial c}{\partial \mathbf{x}}$	$SED := (1-p) \cdot SED$

If a very high energy scaling (e.g. $p = 0.98$) is applied, nearly all of the available material goes to the preferred region and results in a design which looks very similar to the reference design. A completely dissimilar design is obtained by applying a very low scaling value (e.g. $p = 0.02$). It is also important to note that applying a scaling value of $p = 0.5$ is equivalent to running the conventional TO, where similarity control is not addressed. So, the designer is able to get the designs of varying similarity w.r.t. the reference by changing p between nearly 0 and nearly 1.

To evaluate ESM, it is incorporated into the 88-line Matlab code [34] for 2D linear elastic static similarity-driven TO using OC-based SIMP. In order to show that ESM is equally applicable to non-gradient TO methods, ESM is also combined with the HCA approach [30].

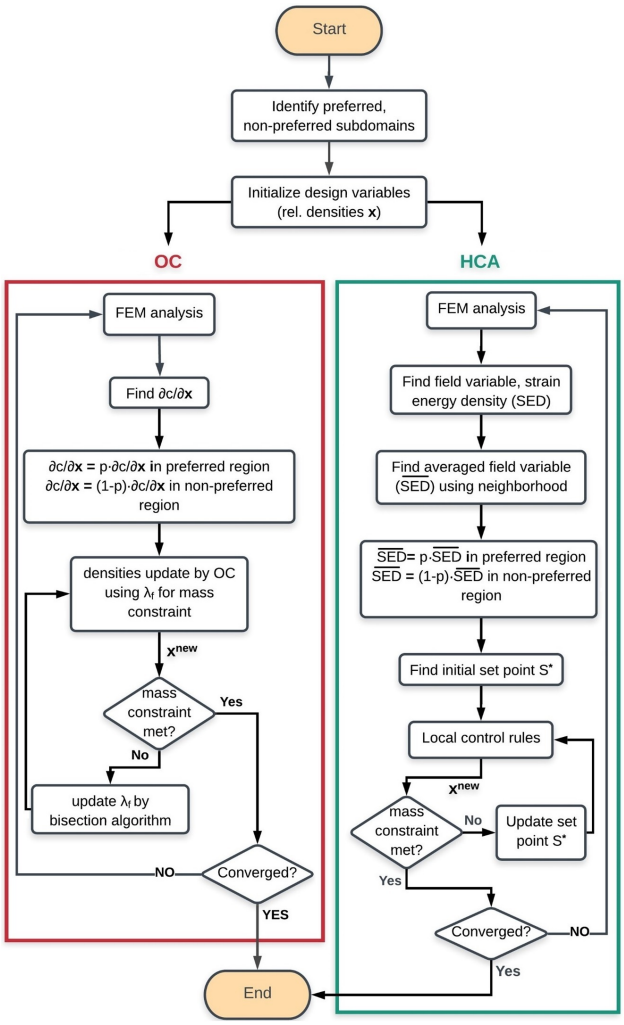

Fig. 2: Similarity-driven TO using ESM in OC-based SIMP and HCA [25].

5 TEST CASES AND RESULTS

In the first test case, we use a 2D square plate under linear elastic static conditions (Fig. 3a). Two variants of this test case are considered. The first variant is used to achieve the following:

1. Compare the similarity-driven TO results of ESM in OC-based SIMP and the formal mathematical approach of OC-based SIMP with similarity constraint.
2. Show that ESM works for both the gradient-based TO like OC-based SIMP and non-gradient TO like HCA. Here, TO is performed by implementing ESM in both methods to achieve global similarity w.r.t. the same reference structure.
3. Demonstrate how the material distribution in the reference structure affects the similarity-driven TO.
4. Investigate the influence of the reference structure on the relationship between the scaling parameter p and the dissimilarity metric s for the optimized design.

On the other hand, the second variant is used to achieve the local/subdomain similarity using ESM in OC-based SIMP.

In the second test case we consider a 2D beam under dynamic nonlinear crash loading conditions. Here, ESM is used in HCA to get the designs of varying similarity w.r.t. a reference design. Moreover, in the third test case, the similarity-driven TO of a 3D frontal hood of a car body is realized by using ESM in HCA to demonstrate its potential for application in the industry.

Finally, as additional application of ESM, a 2D linear elastic test case, similar to the first one, is used to point out the potential of ESM for design domain-based sensitivity analysis in TO.

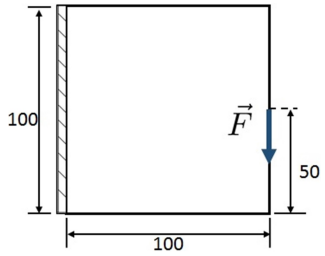

(a) Design space and BCs.

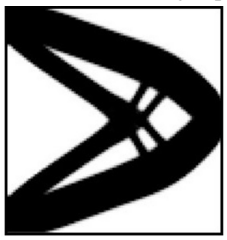

(b) Default TO result using OC-based SIMP.

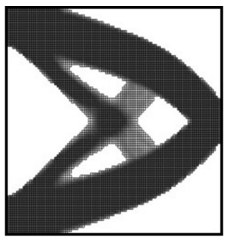

(c) Default TO result using standard HCA.

Fig. 3: Test case of 2D square plate [25].

5.1 Compliance Minimization of a Linear Elastic 2D Square Plate with Global Similarity Control

The first test case is shown in Fig. 3a. It is fixed on the left edge and subject to a unit downward load on the midpoint of the right edge of the design domain. A compliance minimization problem with a volume constraint is considered. The finite element discretization consists of 100×100 square elements of unit dimensions. Here, the similarity in the optimized design is required w.r.t. the reference structure shown in Fig. 1b. The designs obtained with conventional TO using OC-based SIMP and HCA are shown in Fig. 3b and Fig. 3c, respectively. For this, the simulation and optimization parameters given in Table 2 are used. All other TO parameters for OC-based SIMP and HCA are the same as discussed in [34] and [30].

5.1.1 Experimental Procedure

The formal mathematical approach of OC-based SIMP with a similarity constraint [25] is used to perform 14 similarity-driven TO runs to generate designs of dissimilarity metric between 0 and 1 w.r.t. the reference. For ESM, the scaling parameter p is sampled uniformly in the range from 0.02 to 0.98 and 25 sampling points are generated. For each value of p, a complete similarity-driven TO run is performed using ESM in both OC-based SIMP and HCA. Each TO run delivers a design of a certain similarity level w.r.t. the considered reference.

Table 2: Optimization and simulation parameters for OC-based SIMP and HCA for 2D square plate test case [25].

Parameter	OC-based SIMP	HCA
Force magnitude	1 N	0.01 N
Mesh size	100×100	100×100
Element type	4-node shell	4-node shell
Poisson's ratio ν	0.3	0.3
Young's modulus E	1 [MPa]	1 [MPa]
SIMP penalization	3	1
Filter radius	1.5	1.5
Volume fraction	0.5	0.5

5.1.2 Results and Discussion

Fig. 4 compares the similarity-driven TO results of OC-based SIMP with similarity constraint and ESM in OC-based SIMP for the considered test case. The methods are successful in generating a variety of designs. The designs of the highest, intermediate, and the lowest similarity level are represented by the left, center, and the right ends of the curves in Fig. 4. The designer will have to make a compromise between the similarity w.r.t. the reference and the overall performance (compliance) of the obtained design. This is because of the fact that the increase in the similarity level degrades the performance.

As shown in Fig. 4, both methods generate qualitatively similar designs for a given dissimilarity metric value, which demonstrates the correctness of the heuristic energy scaling rule used in ESM. For most of the design concepts obtained using the heuristic ESM, the performance (compliance) is better than those obtained by using the formal mathematical approach of similarity constraint in OC-based SIMP. The performance comparison of the obtained designs with both methods having nearly the same similarity level w.r.t. the reference is given in Table 3. It can be observed that for designs of higher dissimilarity metric value (dissimilar w.r.t. the reference), the performance improvement using ESM is quite large (up to 20.74%). The reason is that the method of similarity constraint in OC-based SIMP fails to converge to 0-1 designs, even for a high value of penalization factor P. This is observable by the grey areas in the designs of high dissimilarity metric values. Similar problem was observed by [26] when using L2-norm for quantification of geometric dissimilarity. On the other hand, ESM is free from

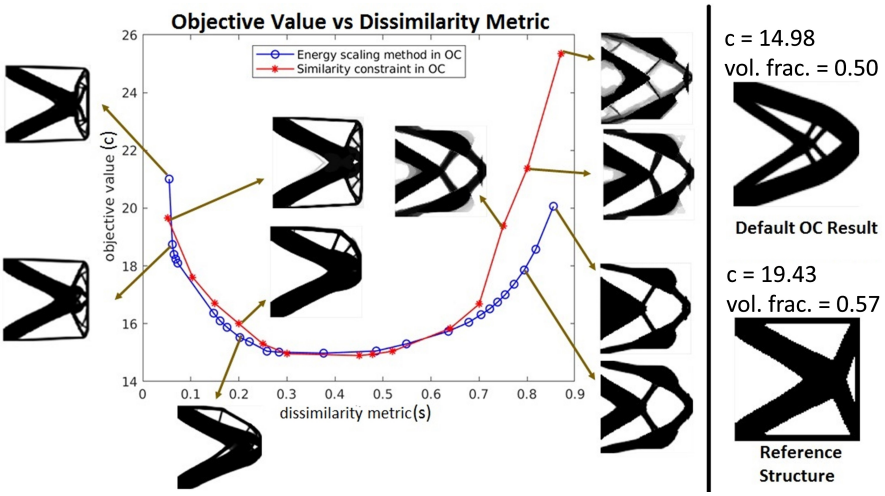

Fig. 4: Similarity-driven TO results using ESM and similarity constraint in OC-based SIMP. The structures with different dissimilarity metric values w.r.t. the reference along with their corresponding objective function (compliance) values are shown [25]. The asymmetry of some structures may result from a small asymmetry of the reference design.

this problem and it always delivers a 0-1 design (even for the default penalization factor of 3). The ESM is also very robust w.r.t. variations of the parameters of the optimization algorithm such as SIMP penalization power or the filter radius. One possible reason for the better quality of designs obtained with ESM is that the same scaling values are applied over larger areas of the design domain and do not change over the optimization iterations, which leads to a higher stability of the algorithm. In contrast, the OC-based SIMP with similarity constraint computes sensitivities for each element independently and adapts them over the course of the optimization, which hinders development of clear boundary between material and void. Considering the computational costs per optimization iteration, both methods perform similarly and are close to the standard OC-based SIMP. This is due to the fact that essentially, the computation of similarity sensitivities or the energy scaling involves only one additional matrix operation, being subtraction or element-wise multiplication, which has a negligible impact on the computational efficiency of the algorithm. Also in terms of convergence velocity of both methods, our experiments have not shown significant differences w.r.t. the standard OC-based SIMP.

Qualitatively similar results were obtained by using ESM in HCA for the test case. The obtained topologies along with their performance and dissimilarity metric values are shown in Fig. 5. The results show that ESM can also be successfully applied in similarity-driven TO with non-gradient TO like HCA. It can be observed that the obtained designs can be regarded as topologically-similar to the ones obtained with ESM in OC-based SIMP.

5.2 Compliance Minimization of a Linear Elastic 2D Square Plate with Local Similarity Control

In the previous test case, ESM was used to control the similarity of the obtained design in the whole design domain w.r.t. the considered reference structure. Now, the capability of the method is shown to control the similarity in just a part of the design domain. This is sometimes required when the designers have precise preferences only in certain subdomains of the whole design domain and they accept any design concept in the other subdomains. There might be another situation where the designers cannot judge whether a certain region should be specified as preferred or non-preferred for similarity control. The test case considered here is the same as shown in Fig. 3a along with the corresponding result in Fig. 3b for compliance minimization TO with default OC-based SIMP. In the upper half subdomain of the test case, similarity control w.r.t. the corresponding subdomain of the reference structure shown in Fig. 1b is imposed by using the ESM in OC-based SIMP (Fig. 6).

5.2.1 Experimental Procedure

Preferred and non-preferred regions are defined only in the upper half subdomain, where the similarity control is required. It is important to mention that no scaling is applied in the lower half subdomain. Furthermore, the dissimilarity metric is computed by taking the mean squared pixel difference in the upper half subdomain of the obtained and the reference design. In total 25, subdomain similarity-driven TO runs are performed by chang-

Table 3: Performance (compliance) improvement (I) for different values of dissimilarity metric (s) by using ESM instead of similarity constraint in OC-based SIMP for similarity-driven TO.

s	0.053	0.15	0.20	0.29	0.48	0.64	0.70	0.75	0.80	0.86
I	-6.9%	2.1%	3.0%	-0.33%	-0.74%	0.63%	2.22%	12.33%	16.42%	20.74%

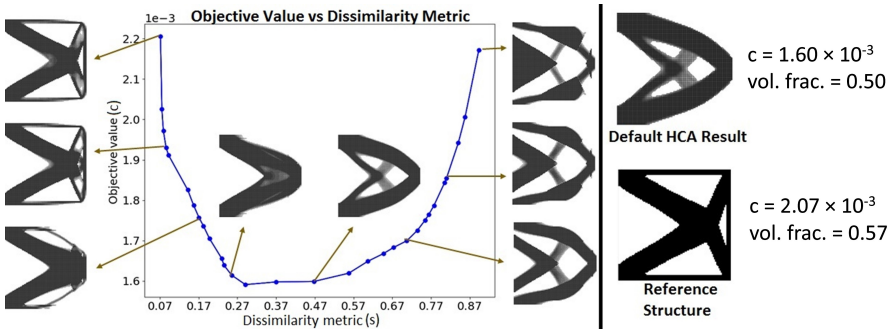

Fig. 5: Similarity-driven TO results using ESM in HCA. The structures with different dissimilarity metric values w.r.t. the reference along with their corresponding objective function (compliance) values are shown [25].

ing the energy scaling p uniformly in the range from 0.02 till 0.98.

5.2.2 *Results and Discussion*

Fig. 6 shows the objective values of different obtained designs. On the left end of the curve, the obtained design has a minimum subdomain dissimilarity metric value (maximum level of local similarity), while the designs on the right end have a high subdomain dissimilarity metric value (minimum level of local similarity) w.r.t. the reference. Furthermore, some oscillations can be observed on the right end. This might be because of the fact that the dissimilarity metric was computed just in the upper half subdomain. It is possible that two designs have the same upper half but the material distribution in the lower half subdomain is different. This will, as a result, deliver designs with nearly the same value of the considered dissimilarity metric, but different objective (performance) values. The obtained results show that ESM is equally good for controlling similarity w.r.t. a reference in a part of the design domain (local similarity).

5.3 2D Beam under Impact Loading

To test ESM for similarity-driven TO with HCA under non-linear dynamic loading conditions, a beam of dimensions $800\text{mm}\times200\text{mm}\times10\text{mm}$ as shown in Fig. 7a is considered. This test case has been considered as a benchmark in literature [11, 35] for 2D TO under impact loading. The beam is fixed on the vertical edges and impacted by a rigid pole of 70mm radius with a specified initial velocity on the top edge at an offset from the midpoint to the left. The FEM model of the test case is shown in Fig. 7b. To make the problem 2D and minimize computational efforts, zero value is specified for the DOFs in the z-direction. The result of TO with conventional HCA without any similarity control is shown in Fig. 7c. For similarity-driven TO, the reference structure of Fig. 7d is considered, which was obtained via TO of a test case where the pole hits the beam right at the center of the top edge. For FEM simulations, piecewise linear plastic (*MAT_PIECEWISE_LINEAR_PLASTICITY LS-DYNA card) and rigid (*MAT_RIGID LS-DYNA card) material model is used for the beam and the pole, respectively. The values for the simulation and optimization parameters are given in Table 4.

5.3.1 *Experimental Procedure*

The scaling value p is sampled uniformly (total 14 samples) in the range from 0.05 to 0.95. For each value of p, similarity-driven TO is performed using ESM in HCA and the performance of the obtained structure is measured by the maximum intrusion of the pole into the beam. The procedure is repeated for three impact velocities of 20m/s, 40m/s, and 60m/s and setting LS-Dyna termination time to 3.0×10^{-3}s, 4.5×10^{-3}s, and 6.0×10^{-3}s, respectively, to allow for a simulation of the entire crash event, i.e.

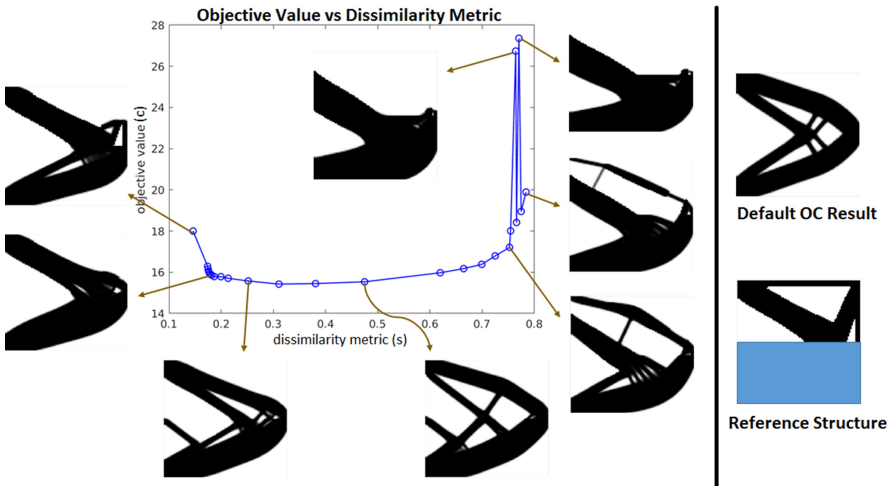

Fig. 6: Objective value (compliance) vs. dissimilarity metric value of the obtained designs for subdomain similarity control study.

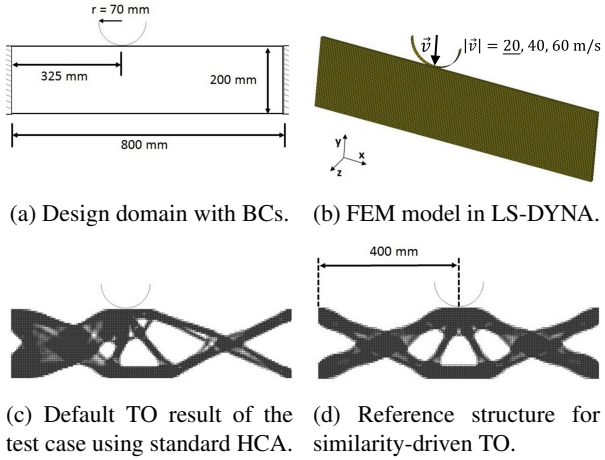

(a) Design domain with BCs.

(b) FEM model in LS-DYNA.

(c) Default TO result of the test case using standard HCA.

(d) Reference structure for similarity-driven TO.

Fig. 7: Test case of 2D beam with fixed edges under impact loading [25].

until the elastic rebound. The discussion of the results is given below.

5.3.2 *Results and Discussion*

Performance (maximum intrusion of the pole) vs. dissimilarity metric results of the similarity-driven TO for the considered test case with pole impact velocity of 20m/s are shown in Fig. 8. As in the previous linear elastic static scenario, ESM also works very well for the dynamic case to deliver designs of different similarity level w.r.t. the reference. The curve in Fig. 8 represents the designs of maximum, intermediate, and minimum similarity w.r.t. the reference on its left end, center, and the right end, respectively. It is also important to note that the maximum similarity level comes at the cost of poor performance. Therefore, the designer should make a proper compromise between the similarity w.r.t. the reference and the overall performance indicator.

The performance vs. dissimilarity metric results for

Table 4: Optimization and simulation parameters for 2D beam test case with impact loading [25].

Parameter	Value
Pole mesh	22 elements
Pole element type	4-node shell
Pole density	5.0×10^{-6} [ton/mm^3]
Beam mesh	$160 \times 40 \times 1$
Beam element type	8-node solid
Beam density	2.7×10^{-9} [ton/mm^3]
Beam Young's modulus E	7.0×10^4 [MPa]
Beam Poisson's ratio ν	0.33
Beam yield strength σ_y	241 [MPa]
Beam tangent modulus E_{tan}	70 [MPa]
Volume fraction	0.5
Filter radius	5.5 [mm]

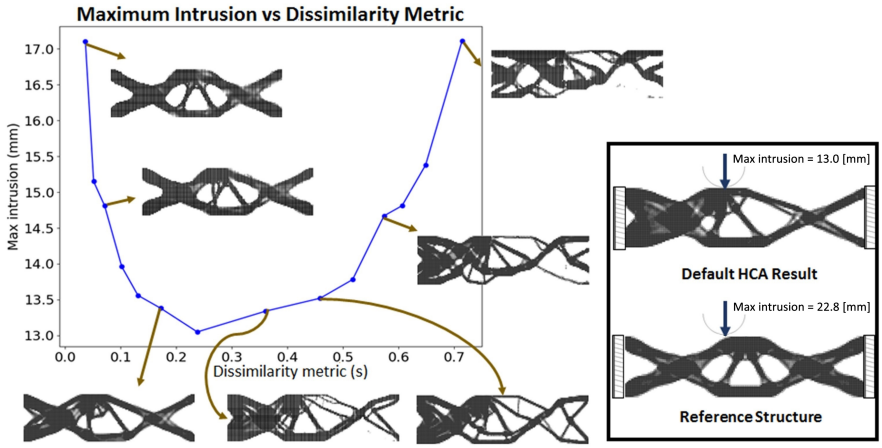

Fig. 8: Performance vs. dissimilarity metric in similarity-driven TO of 2D crash test case for pole impact velocity of 20m/s.

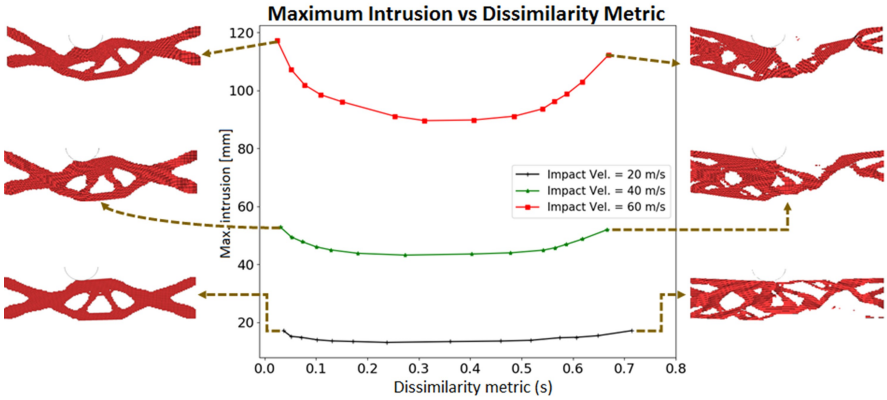

Fig. 9: Effect of impact velocity on performance vs. dissimilarity metric in similarity-driven TO of 2D crash test case. The shown deformed structures are at the moment when the maximum intrusion of the pole happens.

similarity-driven TO with different pole impact velocities are compared in Fig. 9. For each impact velocity, the deformed shape at the moment of the highest intrusion of the pole is also shown for the structures which are the most similar and the most dissimilar to the reference. The maximum intrusion for impact velocity of 60m/s is around 120mm, which is more than half of the beam height. This shows the robustness of ESM for similarity-driven TO under highly non-linear loading conditions.

5.4 Industrial Test Case: Frontal Hood of a Car Body

To further test the capabilities of ESM for similarity control, a large-scale 3D industrial test case is considered. The LS-Dyna model for the test case and the reference structure for similarity control were provided by Honda Development & Manufacturing of America (HDMA). In this test case, stiffness maximization TO of the frontal hood of a car body is performed using HCA. Here, nodes with prescribed displacements are considered to simulate a hood lift related to aerodynamic loads under linear elastic scenario. For a given value of prescribed displacement, the stiffest structure will be the one which will require maximum force to displace the nodes by the prescribed value. This will cause the stiffest structure to have a maximum amount of internal energy under the given BCs.

The design domain and the BCs are shown in Fig. 10. For this test case, ESM in HCA is used to control the similarity w.r.t. the reference structure. The reference structure (defined as the preferred region by the designers at HDMA) is shown in Fig. 11. The volume fraction of this reference structure was 0.76, but practically, such

a high volume fraction is rarely used during TO. Therefore, a volume fraction of 0.35 is used during similarity control experiments. The default HCA result (post-processed to achieve 0-1 design), without any similarity control and obtained with simulation and optimization parameters given in Table 5, is shown in Fig. 12.

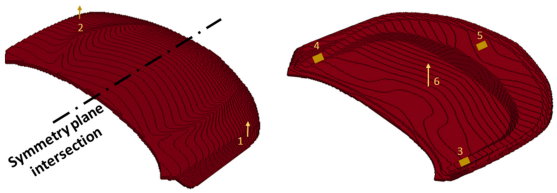

Fig. 10: Design domain used for similarity-driven TO of the industrial test case. 1 and 2: Prescribed displacement BCs. 3 and 4: Fixed support BCs. 5: Pin support BCs. 6: Mass distributed gravity load.

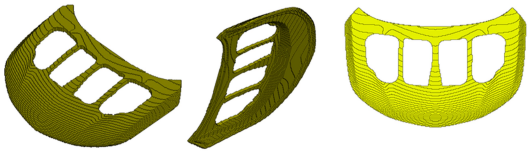

Fig. 11: Considered reference structure views for similarity-driven TO of the industrial test case.

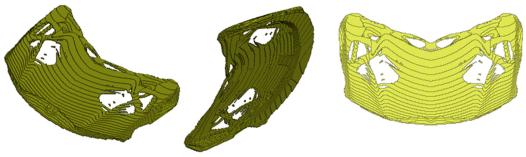

Fig. 12: Default HCA result views (post-processed to 0-1 design) for the industrial case without similarity control.

5.4.1 *Experimental Procedure*

In total, 13 values of energy scaling p are chosen in the range 0.02 to 0.98 and the similarity-driven TO runs using ESM in HCA were performed for each of those values. The results are discussed below.

Table 5: Simulation and optimization parameters for similarity-driven TO of industrial test case.

Parameter	Value
Number of elements	$195,830$
Element type	8-node solid
Prescribed displacement	2 [mm]
Density ρ	2.7×10^{-9} [ton/mm^3]
Young's modulus E	6.7×10^4 [MPa]
Poisson's ratio ν	0.32
Volume fraction	0.35
HCA filter radius	10.5 [mm]
Symmetry constraint	as shown in Fig. 10

5.4.2 *Results and Discussion*

Here, internal energy per unit mass, which can be obtained from LS-Dyna, is used as performance indicator to compare different designs. Fig. 13 shows the similarity-driven TO results for the industrial test case. Once again, ESM has shown to be able to deliver the designs which are highly similar to the given reference structure (Design A: left end of the curve in Fig. 13) or completely dissimilar to it (right end of the curve in Fig. 13). Fig. 13 shows that the minimum possible dissimilarity metric, even for the highest energy scaling value of $p = 0.98$, is around 0.4. The reason for this is the lower target volume fraction value in similarity-driven TO as compared to the reference structure. Due to the smaller amount of available material, no more material can be put in the preferred region to further reduce the voxel difference (dissimilarity metric) between the reference and the obtained design. However, even for this high dissimilarity metric value of 0.4, the corresponding design (Design A) looks very similar to the given reference structure with almost all the material in the preferred region.

The results in Fig. 13 help the designer to identify the new structural components and the design modifications which have to be realized in the reference structure to improve its performance. Design A in Fig. 13 is the most similar to the reference, but it shows a very poor performance value. On the other hand, Design B still looks similar to the reference, but shows a performance improvement of around 10% as compared to Design A. This performance improvement is achieved by building some new structural components in the central region of

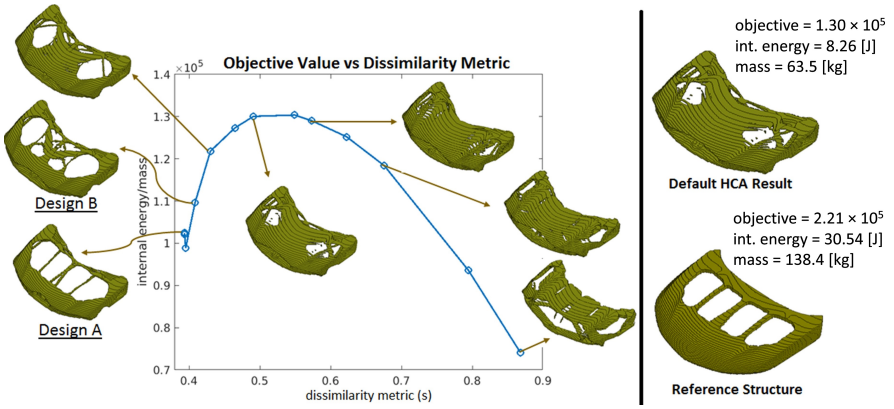

Fig. 13: Performance indicator vs. dissimilarity metric, together with corresponding designs, in similarity-driven TO of the industrial test case.

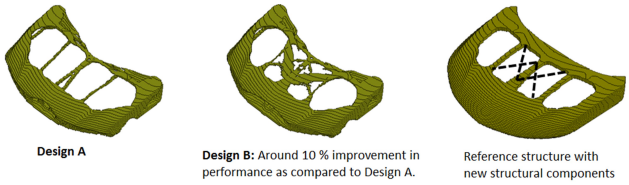

Fig. 14: Performance improvement by realizing some design modifications in the reference structure. These design modifications are obtained by similarity-driven TO using ESM in HCA.

the Design A (Fig. 14). In short, these new structural components can be incorporated in the reference structure to get a better objective function value.

6 INFLUENCE OF THE SCALING PARAMETER

As discussed in Sec. 5, the similarity of the optimized design w.r.t. reference in ESM is controlled by adjusting the scaling parameter p. In the conducted experiments, a sequence of TO runs was always performed for different values of p to explore designs of different similarity levels and select the ones that are the most interesting for the designer. Based on such a sampling, a specific similarity level can be achieved by conducting optimization for an interpolated value of p. However, in industrial setting, where simulations are computationally costly, it might be impractical to run multiple optimizations to determine the scaling factor value for the desired similarity level w.r.t. reference. Hence, it becomes essential to understand the key determinants of the relationship between the dissimilarity metric s in the optimized design and the scaling factor p. In this section, based on a sensitivity study, we determine the features that influence this characteristic, which can help to set the parameter p.

For the four reference designs presented in Fig. 15, we present the curves obtained by running TO using ESM within HCA for different values of p. The optimization settings, parameters of the mechanical model as well as the boundary conditions remain the same as in the experiments in Sec. 5.1. As demonstrated in Sec. 5.1.2, OC-based SIMP and HCA yield similar results when used with ESM and therefore, also the relationships in Fig. 15 look very similar for the OC-based SIMP [36].

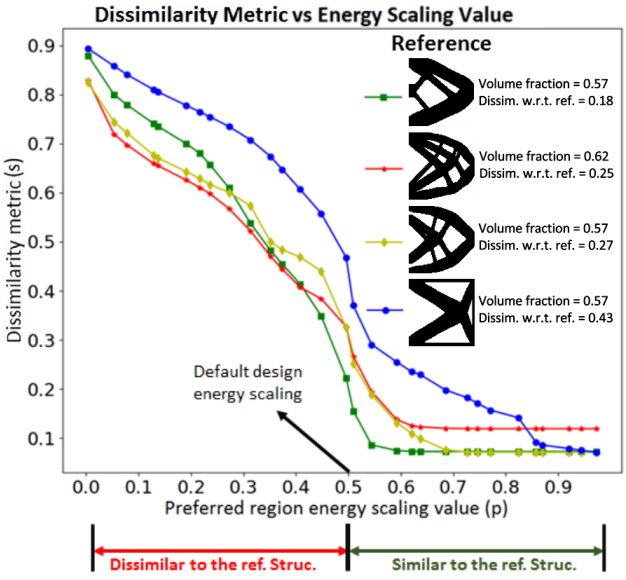

Fig. 15: Relationship between energy scaling factor p and the dissimilarity metric s for structures optimized using ESM in HCA, for four different reference structures.

By analyzing the curves presented in Fig. 15, one can conclude that the following three features influence most strongly the relationship $s(p)$:

1. Target volume fraction.
2. Volume fraction of the reference design – the higher the difference between this quantity and the target volume fraction, the higher is the dissimilarity for $p > 0.5$, which can be seen in case of the red curve.
3. Dissimilarity of the default TO result w.r.t. reference – the lower this value, the lower dissimilarity metric and more flat characteristic is obtained for different values of $p > 0.5$ since ESM influences to a small extent the material distribution. This is visible when comparing the blue curve with the rest of the curves.

Based on the input features described above, it is possible to build a machine learning model capable of accurately predicting the value of scaling parameter p to obtain a specific value of dissimilarity metric in the optimized design for a wide range of TO problems [36]. In such a case, only running the default TO prior to the similarity-based TO is required to predict the value of p. A description of this approach will follow in our future publications.

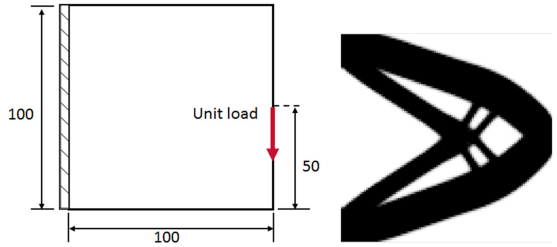

(a) Default design domain. (b) Default OC result.

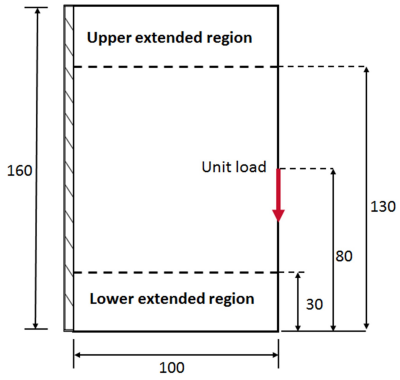

(c) New extended design domain.

Fig. 16: Test case for design domain extension study.

7 DESIGN DOMAIN EXTENSION WITH ESM

In the previous sections, ESM has been shown to be very effective in controlling the similarity of the design obtained after TO w.r.t. a given reference. In this section, the concept of similarity-driven TO is further extended to demonstrate how ESM can be used to study the effect of a change in the design domain dimensions on the overall performance of the obtained design.

During the initial design phase, the interior and the exterior of a vehicle are specified based on styling, aerodynamics, available space, packaging, or other practical design requirements. This results in the definition of the design domain for TO. Conventionally, the design domain is kept fixed and the whole structure is meant to be developed only inside the domain. However, considerable improvement in the overall performance of the obtained design is possible if we allow the material to be present at certain locations in the slightly extended region of the original design domain. Consequently, in case of large benefits coming from the extension of the design domain, the structural engineering department can propose modifications to the other relevant design groups. This study can be seen as a sensitivity analysis of the performance w.r.t. the extension of the design domain. In this article, an extended version of the original design domain is considered and ESM implemented in OC-based SIMP is used to control the material quantity in the outer extended region to get different designs.

7.1 Test Case

A 2D test case (with 100×100 square elements of unit dimensions) with left edge fixed and a unit load on the midpoint of the right edge is considered for compliance minimization TO. The design domain definition and the result for this design domain with default OC-based SIMP of 88 line Matlab code under volume fraction constraint of 0.5 are shown in Fig. 16a and 16b.

A new extended design domain with 100×160 square elements of unit dimensions is considered as shown in Fig. 16c. For the application of ESM, the whole inner region of this new extended design domain is considered as preferred with energy scaling value of p. The upper and lower extended regions are considered as non-preferred regions with the same energy scaling value of $1 - p$.

7.2 Experimental Procedure

Total 24 complete TO runs are performed using the new extended domain (Fig. 16c) for the values of preferred region energy scaling p in the uniform range of 0.02 to 0.98. During all these simulations, the total mass in the final obtained structure is kept the same as in the

design obtained using the original design domain (Fig. 16b). This is achieved by applying a target volume fraction value of 0.31 in the new extended design domain. Furthermore, the dissimilarity metric as discussed previously is also used here to assess the amount of material in the upper and lower extended regions of the obtained design. A design with minimum material in the extended regions will have maximum similarity to the design obtained by using the original design domain.

7.3 Results and Discussion

The objective values (compliance) for the obtained designs of different dissimilarity metric values are shown in Fig. 17. On the right end of the curve, "Design a" has nearly no material in the extended regions and it is the same as the design corresponding to the original domain. On the left curve end, "Design h" has the maximum amount of material in the extended regions and it is a completely new conceptual design. "Design e" is the one which was obtained for $p = 0.5$. This design is the same as the designer would get by using default OC-based SIMP on the extended design domain without using ESM. "Design b" would be perhaps the most interesting for the designer because almost the whole amount of material is still inside the original design domain, but it shows around 7.15% improvement in the objective value. "Design c" shows around 21% improvement in the objective value but it has slightly more material in the extended regions as compared to "Design b". Still, the material that goes in the extended regions is accumulated near the left fixed edge and the rest of the extended regions are empty. This shows that by slightly extending the design domain near the fixed edge of the considered test case, it is possible to considerably improve the performance of the structure.

8 CONCLUSION

In this paper, a novel concept of similarity-driven Topology Optimization (TO) is demonstrated which enables the designer to have more control over the process of TO. A heuristic method for similarity-driven TO called Energy Scaling Method (ESM) is developed by carefully observing the working principles of the formal mathematical method of OC-based SIMP with similarity constraint. The comparison of both methods for linear elastic static similarity-driven TO shows the superiority of ESM. Although both methods are capable of delivering a wide variety of designs by controlling their similarity w.r.t. the reference, the heuristic ESM delivers designs with better performance, specially for the designs of lower similarity level w.r.t. the reference. This makes ESM favorable when the novelty of the obtained designs w.r.t. the reference is important for the designer. Moreover, ESM is also found to be able to generate various designs by controlling their similarity in just a part of the design domain w.r.t. the corresponding part of a given reference.

The implementation of ESM in a certain TO method does not require any sensitivity information. This allows its easy incorporation into gradient methods like OC-based SIMP as well as non-gradient methods like HCA to realize similarity-driven TO. Using HCA as the main TO algorithm, the capabilities of ESM for highly nonlinear dynamic problems are demonstrated by running similarity-driven TO on a 2D beam with fixed edges, impacted by a pole on the top edge.

The simplicity and low computational cost of ESM allows its use for large-scale industrial problems. In this article, similarity-driven TO is performed on a 3D frontal hood of a car body using ESM in HCA. Again, designs of different similarity level w.r.t. the reference are obtained.

A design domain extension study is conducted in linear elastic static TO of a 2D test case. The quantity of material in the extended portions of the design domain is controlled by coupling ESM with OC-based SIMP. It is found that ESM can deliver designs which have a very small amount of material in the extended portion of the domain but have considerably improved performance. These better performing designs are also not much different from the one obtained using the original design domain. These results show the potential of ESM for sensitivity analysis of performance w.r.t. the design domain size. This can change the way TO is used in the industry by making the design process more flexible and cooperative between different design teams.

Finally, the effectiveness of ESM allows the designer to make a compromise between the overall performance and the desired structural layout by expressing their preferences right in the initial phases of product development.

In this work, ESM was used for similarity-driven TO by controlling the energy scaling parameter p. Designs of different dissimilarity metric w.r.t. the reference were obtained by changing p and performing a number of TO runs. An interesting problem, which we are going to address in our future publications, is to predict the required scaling parameter p to obtain a design of a certain dissimilarity metric. In this way, the designer will have to perform only one similarity-driven TO run using the predicted p to obtain the desired structure.

Moreover, this work considers only one reference structure for similarity-driven TO. Practically, the designer might want to control the structural layout of the obtained design w.r.t. a number of different reference structures. This is particularly important when the nov-

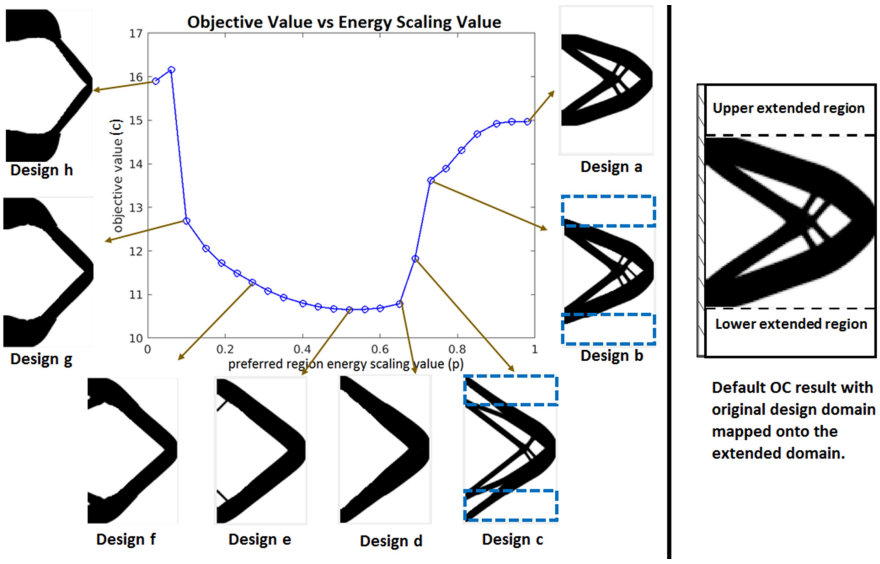

Fig. 17: Objective value vs. energy scaling results for design domain extension study. The dotted lines in designs "b" and "c" show the upper and lower extended regions of the design domain.

elty is important and the new design should be different from the already available designs. Therefore, similarity-driven TO w.r.t. multiple reference structures is also a promising future research direction.

Finally, other dissimilarity metrics, including the ones based on machine learning [37] can also be considered to improve the workflow of similarity-driven TO.

ACKNOWLEDGEMENTS

The authors would like to thank Sanjaya Fonseka (HDMA) for his support in preparing the hood models.

REFERENCES

[1] Bendsøe, M., and Sigmund, O., 2004, *Topology optimization. Theory, methods, and applications.* Springer.

[2] Bendsøe, M. P., and Kikuchi, N., 1988, "Generating optimal topologies in structural design using a homogenization method," *Comput. Methods Appl. Mech. Eng.,* **71**(2), pp. 197–224.

[3] Bendsøe, M. P., 1989, "Optimal shape design as a material distribution problem," *Struct. Optim.,* **1**(4), pp. 193–202.

[4] van Dijk, N. P., Maute, K., Langelaar, M., and van Keulen, F., 2013, "Level-set methods for structural topology optimization: a review," *Struct. Multi. Optim.,* **48**(3), pp. 437–472.

[5] Ma, Y., Chen, X., and Zuo, W., 2020, "Equivalent static displacements method for contact force optimization," *Struct. Multi. Optim.,* **62**, pp. 323–336.

[6] Lu, S., Zhang, Z., Guo, H., Park, G.-J., and Zuo, W., 2021, "Nonlinear dynamic topology optimization with explicit and smooth geometric outline via moving morphable components method," *Struct. Multi. Optim.,* **64**, pp. 2465–2487.

[7] Huang, X., Xie, Y., and Lu, G., 2007, "Topology optimization of energy-absorbing structures," *Int. J. Crashworthiness,* **12**(6), pp. 663–675.

[8] Tovar, A., 2004, "Bone Remodeling as a Hybrid Cellular Automaton Optimization Process," PhD thesis, University of Notre Dame, Indiana, USA.

[9] Duddeck, F., Hunkeler, S., Lozano, P., Wehrle, E., and Zeng, D., 2016, "Topology optimization for crashworthiness of thin-walled structures under axial impact using hybrid cellular automata," *Struct. Multi. Optim.,* **54**(3), pp. 415–428.

[10] Aulig, N., and Olhofer, M., 2016, "State-based representation for structural topology optimization and application to crashworthiness," In 2016 IEEE Congress on Evolutionary Computation (CEC), IEEE, pp. 1642–1649.

[11] Bujny, M., Aulig, N., Olhofer, M., and Duddeck, F., 2018, "Identification of optimal topologies for crashworthiness with the evolutionary level set method," *Int. J. Crashworthiness,* **23**(4), pp. 395–416.

[12] Raponi, E., Bujny, M., Olhofer, M., Aulig, N., Boria, S., and Duddeck, F., 2019, "Kriging-assisted

topology optimization of crash structures," *Comput. Methods Appl. Mech. Eng.,* **348**, pp. 730–752.

[13] Liu, J., and Ma, Y., 2016, "A survey of manufacturing oriented topology optimization methods," *Adv. Eng. Softw.,* **100**, pp. 161–175.

[14] Guo, X., Zhang, W., and Zhong, W., 2014, "Doing topology optimization explicitly and geometrically—a new moving morphable components based framework," *J. Appl. Mech.,* **81**(8).

[15] Norato, J., Bell, B., and Tortorelli, D. A., 2015, "A geometry projection method for continuum-based topology optimization with discrete elements," *Comput. Methods Appl. Mech. Eng.,* **293**, pp. 306–327.

[16] Zhang, W., Chen, J., Zhu, X., Zhou, J., Xue, D., Lei, X., and Guo, X., 2017, "Explicit three dimensional topology optimization via moving morphable void (mmv) approach," *Comput. Methods Appl. Mech. Eng.,* **322**, pp. 590–614.

[17] Zhang, W., Li, D., Zhang, J., and Guo, X., 2016, "Minimum length scale control in structural topology optimization based on the moving morphable components (mmc) approach," *Comput. Methods Appl. Mech. Eng.,* **311**, pp. 327–355.

[18] Zhang, W., Zhou, J., Zhu, Y., and Guo, X., 2017, "Structural complexity control in topology optimization via moving morphable component (mmc) approach," *Struct. Multi. Optim.,* **56**, pp. 535–552.

[19] Bujny, M., Olhofer, M., and Duddeck, F., 2017, "Optimal structures for crash by additive manufacturing," In 1st ECCOMAS Thematic Conf. on Simulation for Additive Manufacturing (Sim-AM).

[20] Guo, X., Zhou, J., Zhang, W., Du, Z., Liu, C., and Liu, Y., 2017, "Self-supporting structure design in additive manufacturing through explicit topology optimization," *Comput. Methods Appl. Mech. Eng.,* **323**, pp. 27–63.

[21] Guo, X., Zhang, W., Zhang, J., and Yuan, J., 2016, "Explicit structural topology optimization based on moving morphable components (mmc) with curved skeletons," *Comput. Methods Appl. Mech. Eng.,* **310**, pp. 711–748.

[22] Zhang, S., Norato, J. A., Gain, A. L., and Lyu, N., 2016, "A geometry projection method for the topology optimization of plate structures," *Struct. Multi. Optim.,* **54**, pp. 1173–1190.

[23] Liu, C., Du, Z., Zhang, W., Zhu, Y., and Guo, X., 2017, "Additive manufacturing-oriented design of graded lattice structures through explicit topology optimization," *J. Appl. Mech.,* **84**(8).

[24] Bai, J., and Zuo, W., 2020, "Hollow structural design in topology optimization via moving morphable component method," *Struct. Multi. Optim.,* **61**(1), pp. 187–205.

[25] Yousaf, M. S., Bujny, M., Zurbrugg, N., Detwiler, D., and Duddeck, F., 2020, "Similarity control in topology optimization under static and crash loading scenarios," *Eng. Optim.,* **53**(9), pp. 1523–1538.

[26] Oh, S., Jung, Y., Kim, S., Lee, I., and Kang, N., 2019, "Deep Generative Design: Integration of Topology Optimization and Generative Models," *ASME J. Mech. Des.,* **141**(11).

[27] Reehuis, E., Olhofer, M., Emmerich, M., Sendhoff, B., and Bäck, T., 2013, "Novelty and interestingness measures for design-space exploration," In 15th Genetic and Evolutionary Computation Conference.

[28] Krish, S., 2011, "A practical generative design method," *Comput. Aided Des.,* **43**(1), pp. 88–100.

[29] Sigmund, O., 2001, "A 99 line topology optimization code written in Matlab," *Struct. Multi. Optim.,* **21**(2), pp. 120–127.

[30] Patel, N. M., Kang, B.-S., Renaud, J. E., and Tovar, A., 2009, "Crashworthiness design using topology optimization," *ASME J. Mech. Des.,* **131**(6), pp. 0610131–06101312.

[31] Bandi, P., Schmiedeler, J. P., and Tovar, A., 2013, "Design of crashworthy structures with controlled energy absorption in the hybrid cellular automaton framework," *ASME J. Mech. Des.,* **135**(9), p. 091002.

[32] Dommaraju, N., Bujny, M., Menzel, S., Olhofer, M., and Duddeck, F., 2023, "Evaluation of geometric similarity metrics for structural clusters generated using topology optimization," *Appl. Intell.,* **53**, pp. 904–929.

[33] Lara Lopez, G., Peña Pérez Negrón, A., De Antonio Jimenez, A., Ramirez Rodriguez, J., and Imbert Paredes, R., 2017, "Comparative analysis of shape descriptors for 3d objects," *Multimed. Tools Appl.,* **76**, pp. 6993–7040.

[34] Andreassen, E., Clausen, A., Schevenels, M., Lazarov, B. S., and Sigmund, O., 2011, "Efficient topology optimization in MATLAB using 88 lines of code," *Struct. Multi. Optim.,* **43**(1), pp. 1–16.

[35] Patel, N., 2007, "Crashworthiness Design Using Topology Optimization," PhD thesis, University of Notre Dame, Indiana, USA.

[36] Yousaf, M. S., 2020, "Structural Layout Preferences in Topology Optimization for Statics and Crash," Master's thesis, TU Munich, Munich, Germany.

[37] Dommaraju, N., Bujny, M., Menzel, S., Olhofer, M., and Duddeck, F., 2019, "Identifying topological prototypes using deep point cloud autoencoder networks," In 2019 ICDMW, IEEE, pp. 761–768.